

Quantum information-based analysis of electron-deficient bonds

Jan Brandejs,^{1,2,*} Libor Veis,^{1,†} Szilárd Szalay,^{3,‡} Gergely Barcza,^{1,3,§} Jiří Pittner,^{1,¶} and Örs Legeza^{3,**}

¹*J. Heyrovský Institute of Physical Chemistry, Academy of Sciences of the Czech Republic, v.v.i., Dolejškova 3, 18223 Prague 8, Czech Republic*

²*Faculty of Mathematics and Physics, Charles University, Prague, Czech Republic*

³*Strongly Correlated Systems “Lendület” Research Group, Institute for Solid State Physics and Optics, MTA Wigner Research Centre for Physics, H-1121 Budapest, Konkoly-Thege Miklós út 29-33, Hungary*

Recently, the correlation theory of the chemical bond was developed, which applies concepts of quantum information theory for the characterization of chemical bonds, based on the multiorbital correlations within the molecule. Here for the first time, we extend the use of this mathematical toolbox for the description of electron-deficient bonds. We start by verifying the theory on the textbook example of a molecule with three-center two-electron bonds, namely the diborane(6). We then show that the correlation theory of the chemical bond is able to properly describe bonding situation in more exotic molecules which have been synthesized and characterized only recently, in particular the diborane molecule with four hydrogen atoms [diborane(4)] and neutral zerovalent s-block beryllium complex, whose surprising stability was attributed to a strong three-center two-electron π bond stretching across the C-Be-C core. Our approach is of a high importance especially in the light of a constant chase after novel compounds with extraordinary properties where the bonding is expected to be unusual.

INTRODUCTION

Recent years have witnessed remarkable interest in application of tools of quantum information theory in chemistry^{1–27}. As a prominent example, the performance of state-of-the-art tensor product methods for electronic structure calculations^{17,28–34} heavily relies on proper manipulation of entanglement^{1,4,6,12,14,17,22}. These include density matrix renormalization group (DMRG) method^{35,36}, which variationally optimizes wave functions in the form of matrix product states (MPS).³⁷

Other important examples represent characterization of electron correlation into its static (strong) and dynamic contributions⁹, automatic (black-box) selection of the active spaces^{1,6,17,23,24,38}, or the self-adaptive tensor network states with multi-site correlators²⁵, all of which harness single- and two-orbital entanglement entropies. Last but not least, correlation measures based on the single- and two-orbital entanglement entropies have also been employed for the purposes of bond analysis^{10,20}.

In the preceding work²⁶, we have presented the very general *correlation theory of the chemical bond* based on multiorbital correlation measures which goes beyond the scope of two-orbital picture. It is able to properly describe multiorbital bonds, and we have demonstrated its performance on a representative set of organic molecules (aliphatic as well as aromatic).

In the present article, we apply this theory to systems with electron-deficient bonds, i.e., to compounds which have too few valence electrons for the connections between atoms to be described as covalent bonds, and which have always fascinated chemists. First we apply the theory to the notoriously known textbook example of the diborane(6)³⁹ molecule (B_2H_6) with two-electron three-center bridge bonds and then also to recently characterized diborane(4)⁴⁰ (B_2H_4) and zero-valent complexes

of beryllium^{41,42}. The neutral form of the latter compound exhibits surprising stability, which was attributed to a strong three-center two-electron π bond stretching across the C-Be-C core⁴¹. Unlike in the previous study²⁶, here we work in the bigger detail in a sense that we also employ eigenstates of multiorbital reduced density matrices, which give us additional insights into the character of bonding.

The article is organized as follows: in Sec. II, we briefly present the studied systems, in Sec. III we review the main concepts of the theory of multiorbital correlations, Sec. IV presents the computational details and Sec. V the results of our calculations which are followed by their discussion, the final Section closes with conclusions.

STUDIED SYSTEMS

Diboranes

In its ground state, diborane(6) (Figure 1a) adopts its most stable conformation with two bridging B-H-B bonds, and four terminal B-H bonds. Its structure was first correctly measured in 1943 from infrared spectra of gaseous samples by an undergraduate student, Longuet-Higgins.^{43,44} Subsequent measurements with electron diffraction confirmed his conclusions⁴⁵, and X-ray diffraction detected further systems with bridging hydrogen bond.⁴⁶ The B-H-B bridging was considered an atypical electron-deficient covalent chemical bond.⁴⁷ Diborane(6) is a prominent example of a molecule with three-center two-electron bonds.⁴⁸ As it is a well studied system, we use its B-H-B linkage as a reference to compare with bond strengths and properties of more complex systems featuring three-center two-electron bonds.

According to quantum-chemical calculations^{49–54}, dif-

ferent species of diborane with less than six hydrogens should exist, also featuring the bridging B-H-B bonds. However, all candidates are short-lived reaction intermediates, difficult to prepare and to identify. Hence, no neutral species has been identified experimentally until 2015, when Chou irradiated diborane(6) dispersed in neon at 3 K with far-ultraviolet light, detecting diborane(4), B_2H_4 (Figure 1b).⁴⁰ This new species with two terminal hydrogen atoms possesses two bridging hydrogen atoms, and so it became the simplest neutral boron hydride identified with such a structural feature.

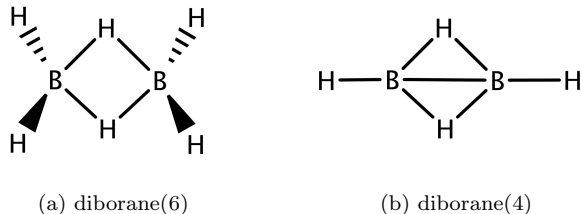


FIG. 1: Structures of diborane(6) and diborane(4).

Beryllium complexes

Complexes of metal atoms of the s-block of the periodic table are often found in their zero oxidation state due to their exceptional electron donation. For their interesting reactivities, these became frequent synthetic targets, competing with traditional transition metal complexes.^{55–57} We follow the recent experimental work of Arrowsmith, who isolated, for the first time, neutral compounds with zero-valent s-block metal, beryllium.⁴¹ These brightly coloured molecules have very short Be-C bonds and beryllium in linear coordination geometries.^{58–61} This indicates strong multiple BeC bonding. According to the theoretical and spectroscopic results, the molecules adopt a closed-shell singlet configuration with a Be(0) metal centre.⁴¹ The complexes are surprisingly stable, and this was ascribed to an unusually strong three-center two-electron π bond stretching across the CBeC unit. Two bonding mechanisms depicted in Figure 2 are taking place, namely σ donation from the carbon doubly occupied sp^2 hybrid orbital to empty s and p_x orbitals on the central Be atom and π back donation from the beryllium p_z orbital to p_z orbitals located on C atoms.

We studied two of the proposed systems. First the $Be(CAC)_2$ complex (Figure 6a), where CAC corresponds to cyclic amino carbene donors, which stabilize the compound due to their π -acidity.^{62,63} We performed a multireference calculation, in order to verify the proposed singlet configuration with a Be(0) metal centre and to provide a deeper insight into the bonding scheme. Next we studied dication $[Be(CAC)_2]^{2+}$ (Figure 6b), in which

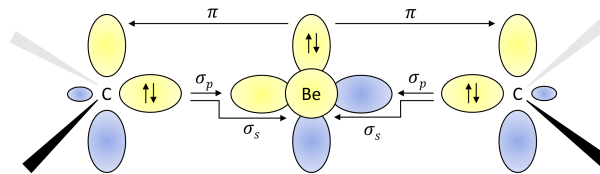


FIG. 2: Schematic representation of the C-Be-C bonding mechanisms⁴¹.

the removal of two electrons disrupts the bridging CBeC bond. This allowed us to compare with the former system and to determine the stabilization effect of the bridging bond.

METHODOLOGY

Recently, the correlation theory of the chemical bond²⁶ was developed, characterizing bonds based on the correlations among orbitals localized on individual atoms. Simply put, if we think of a simple covalent bond and localize the bonding and antibonding molecular orbitals into their atomic contributions, these localized orbitals will be highly correlated. Therefore, standard two-orbital bonds can be characterized by pairs of strongly correlated localized orbitals, and the strength of the correlation characterizes the strength of the bond from the quantum information theoretical point of view.

The correlation theory of the chemical bond can also be used for the characterization of bonds more involved than the covalent bonds. The concept in general is to find the finest possible correlation based clustering of the localized orbitals into clusters, so that the clusters are weakly correlated with each other, and the orbitals inside the clusters are strongly correlated.²⁶ These clusters then form independent bonds of a Lewis structure of a given molecule and the strength of the correlation with respect to this clustering refers to the validity of such a representation. The weaker the correlation is, the better the Lewis structure represents bonding.

In order to review the correlation measures⁶⁴, which will be used in our analysis, let us denote the set of (the labels of) localized orbitals with M . We aim at investigating the correlations in an $L \subseteq M$ set of orbitals (cluster). The state of the full electronic system of the cluster L is given by the density operator ϱ_L , while the reduced state of a (sub)cluster $X \subseteq L$ is given by the reduced density operator ϱ_X in general.^{65–67} If the cluster of orbitals L can be given by a state vector $|\psi_L\rangle$ (for example, when a given eigenstate of the whole molecule is considered), then its density operator is of rank one, $\varrho_L = |\psi_L\rangle\langle\psi_L|$, called a pure state. Its reduced density operator is usually mixed (not of rank one), which is the manifestation of entanglement⁶⁸ between (sub)cluster X and the rest of the cluster $L \setminus X$. In general, a density operator ϱ_X can be decomposed in infinitely many ways into state vectors

$|\psi_i\rangle$ with mixing weights $p_i \geq 0$ as $\varrho_X = \sum p_i |\psi_i\rangle \langle \psi_i|$. The spectral decomposition (where the weights are the λ_i eigenvalues, and the $|\psi_i\rangle$ -s are eigenvectors, being *orthogonal*) is a special one, in the sense that its weights are the least mixed.^{69,70} Each eigenvector $|\psi_i\rangle$ can be expanded in the occupation number basis, the square of the absolute value of the coefficients are the weights of the given occupations in that given eigenvector $|\psi_i\rangle$ of weight λ_i .

On the first level, the correlation is defined with respect to a partition⁷¹ of the L set of the orbitals,^{26,64,72,73} denoted with $\xi = \{X_1, X_2, \dots, X_{|\xi|}\} \equiv X_1|X_2|\dots|X_{|\xi|}$, where the clusters $X \in \xi$, called parts, are disjoint subsets of the cluster L , and $\cup_{X \in \xi} X = L$. The measure of correlation among the parts $X \in \xi$ is the ξ -correlation,^{26,64}

$$C(\xi) := \sum_{X \in \xi} S(X) - S(L). \quad (1)$$

Here $S(X) = -\text{tr}(\varrho_X \log_4 \varrho_X)$ is the von Neumann entropy.^{65,67} (Note that we use the logarithm to the base 4, which is the dimension of the Hilbert space of an orbital. The resulting numerical values are then the same as of the original measures with natural logarithm²⁶ given in the units of $\ln 4$. Note that $S(X) \leq |X|$, where $|X|$ is the number of orbitals in cluster X .) As a special case, the correlation of two single orbitals,

$$C(i|j) = S(i) + S(j) - S(i, j) = I(i|j), \quad (2)$$

is the well-known (two-orbital) mutual information,^{65,67,74} which has already been considered in chemistry.^{6,10–13,16,18–20,26,75–79} (For convenience, we omit the curly brackets $\{ \}$ in the cases when this does not cause confusion.) For a general partition ξ , we have the bound²⁶

$$C(X|Y) \leq 2(|L| - \max_{X \in \xi} |X|), \quad (3a)$$

which for a bipartition $\xi = X|Y$ reduces to

$$C(X|Y) \leq 2 \min\{|X|, |Y|\}. \quad (3b)$$

Note that $C(\xi)$ is zero for the trivial split $\xi = \top = \{L\}$, and it takes its maximum, $C(\perp)$, for the finest split $\xi = \perp = \{\{i\} : i \in L\}$. The latter quantity is also called total correlation,^{2,80–83}

$$C_{\text{tot}}(L) := C(\perp) = \sum_{i \in L} S(i) - S(L). \quad (4)$$

(Note that if cluster L is described by a pure state then $S(L) = 0$, and the correlation is entirely quantum entanglement.^{64,68,84} Moreover, the correlation in a pure state with respect to a bipartition $\xi = X|(L \setminus X)$ is just two times the usual entanglement entropy^{67,85,86}

$$C(X|(L \setminus X)) = 2S(X) = 2S(L \setminus X), \quad (5)$$

because of the Schmidt decomposition of pure states.^{67,86,87}

On the second level, the correlations can be defined in an overall sense, that is, without respect to a given partition.^{26,64,73} The k -partitionability correlation and the k -producibility correlation, are²⁶

$$C_{k\text{-part}}(L) := \min_{\xi: |\xi| \geq k} C(\xi), \quad (6a)$$

$$C_{k\text{-prod}}(L) := \min_{\xi: \forall X \in \xi, |X| \leq k} C(\xi), \quad (6b)$$

for $1 \leq k \leq |L|$. These characterise the strength of two different (one-parameter-) notions of multiorbital correlations; those which cannot be restricted inside at least k parts, and those which cannot be restricted inside parts of size at most k , respectively.²⁶

For the cluster L , as special cases, $C_{|L|\text{-part}} = C_{1\text{-prod}} = C(\perp)$ grabs all the correlations, it is zero if and only if there is no correlation at all in the cluster L . On the other hand, $C_{2\text{-part}} = C_{(|L|-1)\text{-prod}}$ is sensitive only for the strongest correlations, it is nonzero if and only if the cluster L is globally correlated. Note also that $C_{1\text{-part}} = C_{|L|\text{-prod}} = C(\top) = 0$, by definition. Beyond these, there are no such coincidences among the partitionability and producibility correlations for other values of k , however, the relation $C_{k\text{-part}} \geq C_{(|L|-k+1)\text{-prod}}$ holds.²⁶ Also, the following (non strict) bounds hold²⁶

$$C_{k\text{-part}} \leq 2(k-1), \quad (7a)$$

$$C_{k\text{-prod}} \leq 2(|L| - k). \quad (7b)$$

COMPUTATIONAL DETAILS

In case of diborane molecules, the ground state geometries were optimized with the B3LYP/cc-pVDZ method. For the multiorbital correlation studies, the Pipek-Mezey⁸⁸ localized HF/STO-3G molecular orbitals (MOs) were employed^{20,26} and they were manually hybridized (rotated) to better reflect the chemical environment. The quantum chemical (QC-) DMRG method was applied to study the multiorbital correlations in the full orbital following the procedure outlined in Ref. 26.

The ground state geometries of both forms of the beryllium complex, namely $\text{Be}(\text{CAC})_2$ and $[\text{Be}(\text{CAC})_2]^{2+}$ were taken from Ref. 41 and they correspond to the BP86/def2-TZVPP level of theory. Due to the size of the problem, multiorbital correlation studies by means of QC-DMRG are not feasible in the full orbital space. We have rather chosen a different strategy. Since we were interested only in the bonding of the C-Be-C atomic core, we have selected the complete active space (CAS) of relevant orbitals participating or influencing these bonds. In particular, $2p_x$ orbitals on both C and Be atoms and $2s$ orbital on Be, all of them contributing to the σ bonds and $2p_z$ orbitals on both C and neighbouring N atoms and Be, forming or directly influencing the π bonds. The CAS orbitals were optimized by means of the CASSCF(10,9)/cc-pVDZ method in case of the neutral complex and CASSCF(8,9)/cc-pVDZ method in case of

the dication and again localized using the Pipek-Mezey⁸⁸ procedure. They were not hybridized in order to directly compare with the previous work⁴¹ making conclusions about atomic-like orbitals.

All the quantum chemistry calculations except the QC-DMRG ones were performed with the MOLPRO package⁸⁹. The QC-DMRG calculations were carried out using the Budapest QC-DMRG code⁹⁰. Molecular orbitals were visualized with Charmol⁹¹.

RESULTS

The results on diborane(6) are summarized in Figure 3 and Table I, whereas results on diborane(4) are presented in Figure 4 and Table II. All the Figures depict mutual information of pairs of localized orbitals, defined in 2, while the Tables contain numeric values of measures of the relevant kinds of multiorbital correlations, which are discussed below.

In a similar fashion, the results on beryllium complexes are presented in Figures 5, 7, and 8 and Table III.

In the Figures, individual localized orbitals are represented as black dots and dashed blue lines encircle orbitals belonging to one atom. The mutual information is plotted as grayscale edges between the orbitals. Black lines correspond to the strongest correlations, while light gray lines connect the weakly correlated orbitals. Based on the mutual information structure, the orbitals are grouped into strongly correlated clusters, which in our examples correspond to either core orbitals or chemical bonds. The clusters are encircled by red borders.

DISCUSSION

Diborane(6)

Figure 3 shows that our results fit well the established bonding picture of diborane(6) with two bridging B-H-B bonds. Let us now discuss in detail how the analysis of correlations leads to the clustering and to the bonding picture presented in Figure 3. We will discuss only the bridging bonds, the core orbitals as well as terminal B-H bonds are well separated, i.e. not correlated with the rest. (This is confirmed by the weak correlation $C(X_1 \cup X_2 | \text{rest})$ in Table I.)

First we consider the cluster X_1 containing sp^3 hybrid orbitals on B atoms and $1s$ orbital on the bridging H atom. Because of the point group symmetry, the same results hold for cluster X_2 . As can be seen in Table I, the correlation (entanglement) of X_1 with the remaining orbitals is very weak, only 8.6% of the maximum value, which indicates that X_1 forms an independent three-center bond.

However, to confirm this conclusion, we have to show that X_1 cannot be split further. If we take separate pairs of orbitals from X_1 and measure the correlation with

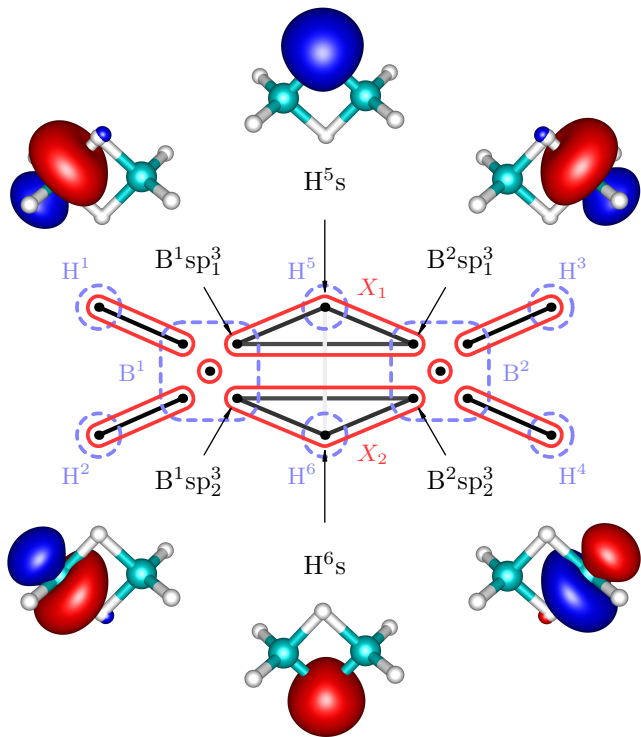


FIG. 3: Schematic view of diborane(6) with mutual information: each dot represents a localized orbital, dashed blue line encircles individual atoms, edges correspond to mutual information (plot shaded by a logarithmic scale depending on strength) and red circles show how the orbitals group into clusters, i.e. independent bonds. Sorted values of the two-orbital mutual information are plotted in Appendix A.

correlation	abs. value	rel. value
$C(X_1 \text{rest})$	0.515	8.6%
$C(X_1 \cup X_2 \text{rest})$	0.412	3.4%
$C(B^1sp_1^3, H^5s \text{rest})$	1.852	46%
$C(H^5s, B^2sp_1^3 \text{rest})$	1.852	46%
$C(B^1sp_2^3, B^2sp_1^3 \text{rest})$	2.114	53%
$C(B^1sp_1^3 H^5s)$	0.894	45%
$C(H^5s B^2sp_1^3)$	0.894	45%
$C(B^1sp_1^3 B^2sp_1^3)$	0.605	30%
$C_{2\text{-part}}(X_1)$	1.500	75%
$C_{3\text{-part}}(X_1)$	2.394	60%
$C(X_1 X_2)$	0.309	5.2%
$C(H^5s H^6s)$	0.042	2.1%

TABLE I: Correlation measures for diborane(6). Relative values are related to the upper bounds. Labeling of localized orbitals corresponds to Figure 3.

the remaining orbitals, we obtain significantly higher values, in particular 46% and 53% of the maximum values

(see Table I), which justifies existence of the three-center bond.

The mutual information of pairs of orbitals within X_1 reach rather small relative values (45%, 30%, see Table I), however according to our numerical experience, even strong multicenter bonds typically yield low percentage, never approaching near the theoretical maxima.²⁶ Intuitive perspective suggests that the correlation of one orbital with the others can be thought of as a resource shared among the orbitals. In other words, all the pairs inside X_1 cannot reach the maximum simultaneously, bounded by entanglement monogamy.^{92,93} The formulation of an inequality bounding the mutual correlations inside orbital clusters still remains an open problem, to our best knowledge. The smaller value of the mutual information between sp^3 hybrid orbitals on B atoms reflects their larger internuclear distance.

We employ k -partitionability in order to quantify and benchmark the strength of the diborane(6) three-center bonds (in terms of correlation). As can be seen in Table I, $C_{2\text{-part}}(X_1)$ reaches 75% of the upper bound and $C_{3\text{-part}}(X_1)$ 60%, which points at a strong bond in X_1 .

The very weak correlation (entanglement) of X_1 with the remaining orbitals also indicates that the state of the cluster X_1 is close to a pure state. Indeed, the eigenstate analysis of the reduced density operator ρ_{X_1} shows that there is the following two-electron eigenstate with a corresponding eigenvalue (probability) of 0.94

$$\begin{aligned}
 |\psi_{X_1}\rangle = & \\
 & + 0.2146 |-- \uparrow\downarrow\rangle + 0.4313 |-\uparrow\downarrow -\rangle + 0.2146 |\uparrow\downarrow --\rangle \\
 & + 0.3787 |-\downarrow\uparrow\rangle - 0.3787 |-\uparrow\downarrow\rangle + 0.2721 |\downarrow -\uparrow\rangle \\
 & + 0.3787 |\uparrow\downarrow -\rangle - 0.3787 |\downarrow\uparrow -\rangle - 0.2721 |\uparrow -\downarrow\rangle,
 \end{aligned}$$

where the ordering of orbitals in a ket corresponds to B^1sp^3 , H^51s , and B^2sp^3 . Other eigenstates have probabilities below 0.01. The principal two-electron eigenstate together with the above discussion on correlations imply that the three orbitals of X_1 form a three-center two-electron bond. Note that the electron pair exhibits a preferred occupation on H atom, which is due to its higher electronegativity when compared to B, as we can see from the principal eigenstate. It is in agreement with the expectation values of particle-number-operators ($\langle\psi|\hat{n}_{el}^{(i)}|\psi\rangle$) which for B^1sp^3 , H^51s and B^2sp^3 equal 0.53, 0.95 and 0.53, respectively.

As one can observe in Table I, the main source of correlation between X_1 and the remaining orbitals is the correlation with the other three-center bond, X_2 . Specifically, the correlation between two bridging H atoms is the strongest, which is caused by higher electron density on these atoms.

Diborane(4)

In case of diborane(4), the two terminal H atoms are missing and instead a direct covalent bond connecting

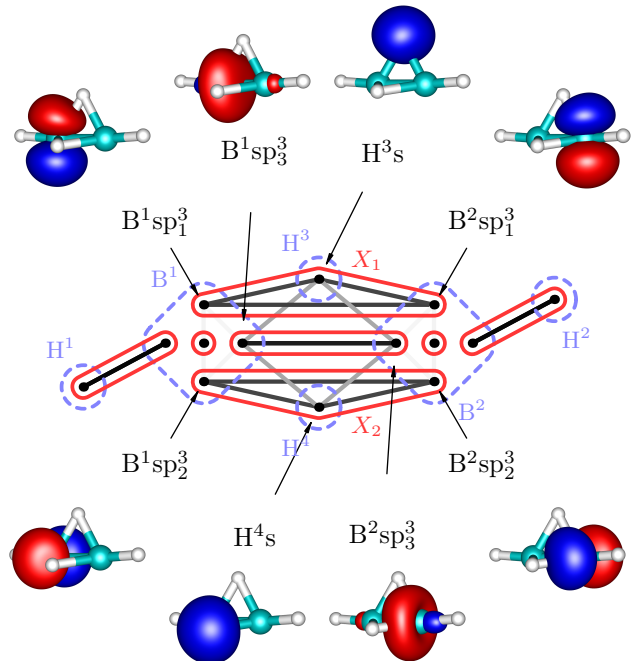


FIG. 4: Schematic view of diborane(4) with mutual information: each dot represents a localized orbital, dashed blue line encircles individual atoms, edges correspond to mutual information (plot shaded by a logarithmic scale depending on strength) and red circles show how the orbitals group into clusters, i.e. independent bonds. Sorted values of the two-orbital mutual information are plotted in Appendix A.

correlation	abs. value	rel. value
$C(X_1 \text{rest})$	1.328	22%
$C(B^1sp_1^3 H^3s)$	0.647	32%
$C(B^1sp_1^3 B^2sp_1^3)$	0.701	35%
$C_{2\text{-part}}(X_1)$	1.388	69%
$C_{3\text{-part}}(X_1)$	2.089	52%
$C(X_3 \text{rest})$	1.438	36%
$C(B^1sp_3^3 B^2sp_3^3)$	1.245	62%
$C(B^1sp_3^3 H^3s)$	0.130	6.5%
$C(X_1 \cup X_2 \cup X_3 \text{rest})$	0.535	6.7%
$C(X_1 X_2)$	0.066	1.1%
$C(X_1 X_3)$	0.639	16%

TABLE II: Correlation measures for diborane(4).

Relative values are related to the upper bounds. Labeling of localized orbitals corresponds to Figure 4.

both B atoms is present⁴⁰. This is also the picture resulting from our analysis and depicted in Figure 4. In comparison to diborane(6), we have the similar three-

orbital clusters X_1 and X_2 , but also the two-orbital cluster X_3 containing sp^3 hybrid orbitals on B atoms and corresponding to the aforementioned B-B bond.

Considering the cluster X_1 , one can observe in Table II that it is more correlated with the remaining orbitals than in case of diborane(6). The value of $C(X_1 | \text{rest})$ is more than two times larger, but the picture of X_1 as a standalone chemical bond is still justifiable. Consequently, the reduced density operator ρ_{X_1} is more mixed, with the principal eigenvalue 0.7803. The remaining eigenstates share low probabilities (below 0.081), and therefore, the picture of X_1 as a standalone chemical bond is still a reasonable qualitative description. The principal eigenstate is again two-electron, i.e. electron-deficient, and it has the following form

$$\begin{aligned} |\psi_{X_1}\rangle = & \\ & - 0.2287 |-- \uparrow\downarrow\rangle - 0.3671 |-\uparrow\downarrow -\rangle - 0.2287 |\uparrow\downarrow --\rangle \\ & + 0.3823 |-\downarrow\uparrow\rangle - 0.3823 |-\uparrow\downarrow\rangle - 0.2967 |\downarrow - \uparrow\rangle \\ & + 0.3823 |\uparrow\downarrow -\rangle - 0.3823 |\downarrow\uparrow -\rangle + 0.2967 |\uparrow - \downarrow\rangle. \end{aligned}$$

Similarly to diborane(6), higher electron density is on the bridging H atom, which is due to its higher electronegativity.

Comparing the two-orbital correlations inside X_1 with diborane(6) (Tables I and II), one can see a weaker correlation between sp^3 hybrid orbitals on B atoms and H 1s orbital, but a slightly stronger correlation between both B-atom-orbitals. This stronger correlation can be certainly assigned to a shorter distance of B atoms (1.477Å vs. 1.784Å). Based on the values of $C_{2\text{-part}}(X_1)$ and $C_{3\text{-part}}(X_1)$, the covalent bond corresponding to the cluster X_1 is slightly weaker (in terms of correlation) than the same bond in diborane(6).

For the cluster $X_3 = \{B^1sp_3^3, B^2sp_3^3\}$, correlation with the remaining orbitals is stronger than for X_1 and X_2 , which in turn weakens the internal two-orbital correlation. The major contribution to the correlation of X_3 with the remaining orbitals originates from $C(B^1sp_3^3 | H^3s)$, which is still very weak compared to other correlations in the molecule (see Table II).

The overall correlation of the three bonding clusters X_1 , X_2 , and X_3 with the rest of the system is similarly weak as in diborane(6) so the considered bonding can be described independently of the rest of the molecule.

Beryllium complexes

In order to check how well our bonding picture of $\text{Be}(\text{CAC})_2$ fits the one proposed by Arrowsmith *et al.*⁴¹, we consider the clusters X_1 and X_2 from Figure 5. The cluster X_1 contains p_z orbitals on C and Be atoms and corresponds to the suggested three-center two-electron π bond, whereas the cluster X_2 contains C p_x orbitals and Be s and p_x orbitals and corresponds to the σ bonds.

Let us start with X_1 . In Table III, one can see that the correlation of X_1 with the remaining orbitals is higher

than 30% of the maximum value, which means that the picture of the three-orbital C-Be-C π bond might be good as a qualitative description, but for a quantitatively adequate description, we might seek to include further orbitals into X_1 , as shown below. This is also demonstrated by weaker pairwise correlations within X_1 , especially $C(C^1p_z | C^2p_z)$, than in the three-orbital bonds discussed above. The correlations of the internal pairs in X_1 with the remaining orbitals are large (61% and 86%) and clearly cannot be considered as standalone bonds.

The inaccuracy of the picture of a standalone three-orbital bond is also demonstrated by the reduced density operator ρ_{X_1} (see in Appendix A), which is much more mixed than in previous cases. It has three dominant eigenvalues, instead of just one. The most significant, nevertheless, corresponds to the two-electron state, which is in agreement with the overall picture of the three-orbital two-electron bond.

correlation	abs. value	rel. value
$C(C^1p_z, C^2p_z \text{rest})$	3.424	86%
$C(C^1p_z, \text{Be } p_z \text{rest})$	2.432	61%
$C(X_1 \text{rest})$	2.032	34%
$C(C^1p_z C^2p_z)$	0.194	9.7%
$C(C^1p_z \text{Be } p_z)$	0.681	34%
$C_{2\text{-part}}(X_1)$	1.153	58%
$C_{3\text{-part}}(X_1)$	1.834	46%
$C(X_1 N^1p_z)$	0.915	46%
$C(X'_1 \text{rest})$	0.209	2.6%
$C(N^1p_z, C^1p_z \text{rest of } X'_1)$	1.737	43%
$C(N^1p_z C^1p_z)$	0.560	28%
$C(X_2 \text{rest})$	0.209	2.6%
$C(C^1p_x \text{Be } s)$	0.765	38%
$C(C^1p_x \text{Be } p_x)$	0.771	39%
$C_{2\text{-part}}(X_2)$	1.936	97%
$C(C^1p_x \text{Be } sp_2)$	1.912	96%

TABLE III: Correlation measures for $\text{Be}(\text{CAC})_2$.

Relative values are related to the upper bounds.

Labeling of localized orbitals corresponds to Figure 5.

As can be seen in Figure 5, the strongest external correlation of X_1 is $C(X_1 | N^1p_z)$. It results from a conjugation of p_z orbitals and has a stabilization effect. Notice that the $N^1\text{-C}^1\text{-Be-C}^2\text{-N}^2$ group of atoms form perfectly planar structure (the dihedral angle $\alpha_{N^1\text{-C}^1\text{-C}^2\text{-N}^2} = 179.97^\circ$) enabling an efficient overlap of all p_z orbitals, which is necessary for the aforementioned conjugation.

The more accurate bonding picture can thus be obtained by considering the enlarged cluster X'_1

$$X_1 \mapsto X'_1 \equiv X_1 \cup \{N^1p_z, N^2p_z\}.$$

The corresponding structure of $\text{Be}(\text{CAC})_2$ is depicted in Figure 6a. The cluster X'_1 is independent of the rest of the molecule. This follows from the negligible correlation

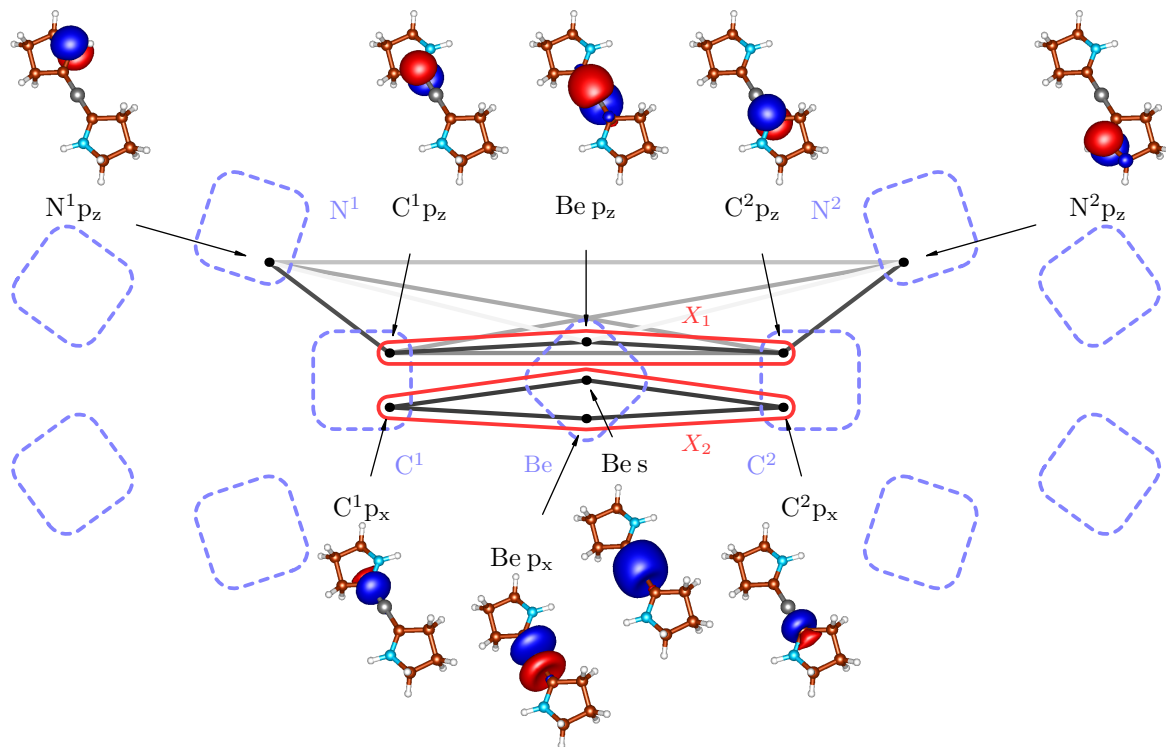


FIG. 5: Schematic view of $\text{Be}(\text{CAC})_2$ with mutual information. In order to be consistent with Figures 3 and 4, all the atoms are depicted (dashed blue line circles), even though only a subset of orbitals (black dots) formed the complete active space. Note that one ring is artificially flipped for clearer correlation picture. Sorted values of the two-orbital mutual information are plotted in Appendix A.

of X'_1 with the remaining orbitals (see Table III). Employing the standard notation, the π electron bond can be denoted as Π_5^6 , i.e. six-electron (two electrons from the Be atom and two from each N atom lone pair) five-center bond, which is confirmed by the particle number expectation value of 6.003.

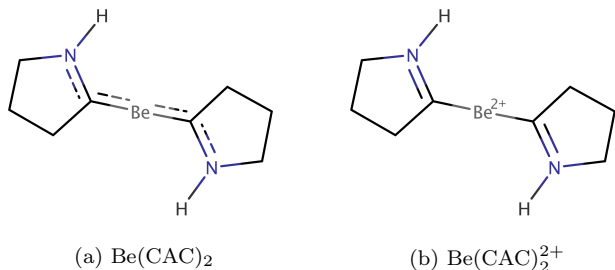


FIG. 6: Structures of studied beryllium complexes suggested by our correlation analysis.

In order to verify the suggested π back-donation mechanism⁴¹, or in other words probe the local electronic configuration of the Be atom, we have also performed

the correlation analysis for the dication $[\text{Be}(\text{CAC})_2]^{2+}$. As can be seen in Figure 7, the difference between the correlation picture of $\text{Be}(\text{CAC})_2$ and $[\text{Be}(\text{CAC})_2]^{2+}$ are almost missing correlations inside the cluster X_1 , which is for example demonstrated by the negligible value of $C_{2\text{-part}}(X_1) = 0.093$. Also the reduced density operator ρ_{X_1} is highly mixed and without the dominating two-electron eigenstate (see in Appendix A). On the other hand, the correlations in the cluster X_2 remain practically unchanged.

This is in agreement with the picture of Be atom having originally two electrons in the p_z orbital. When the C-Be-C bond is formed, they are shared with C-atom p_z orbitals through the back donation mechanism, as is depicted in Figure 2. These two π electrons are missing in case of the dication and the aforementioned π bond is clearly not formed.

Another feature of the correlation picture from Figure 7 is that there are considerably stronger pairwise correlations between C and N-atom p_z orbitals $[C(N^1 p_z | C^1 p_z) = 1.691]$. They are indeed of the strength of donor-acceptor bonds⁹⁴. We thus assign double bonds between N and C atoms to the dication, as is depicted in Figure 6b. The π bonds are formed from the

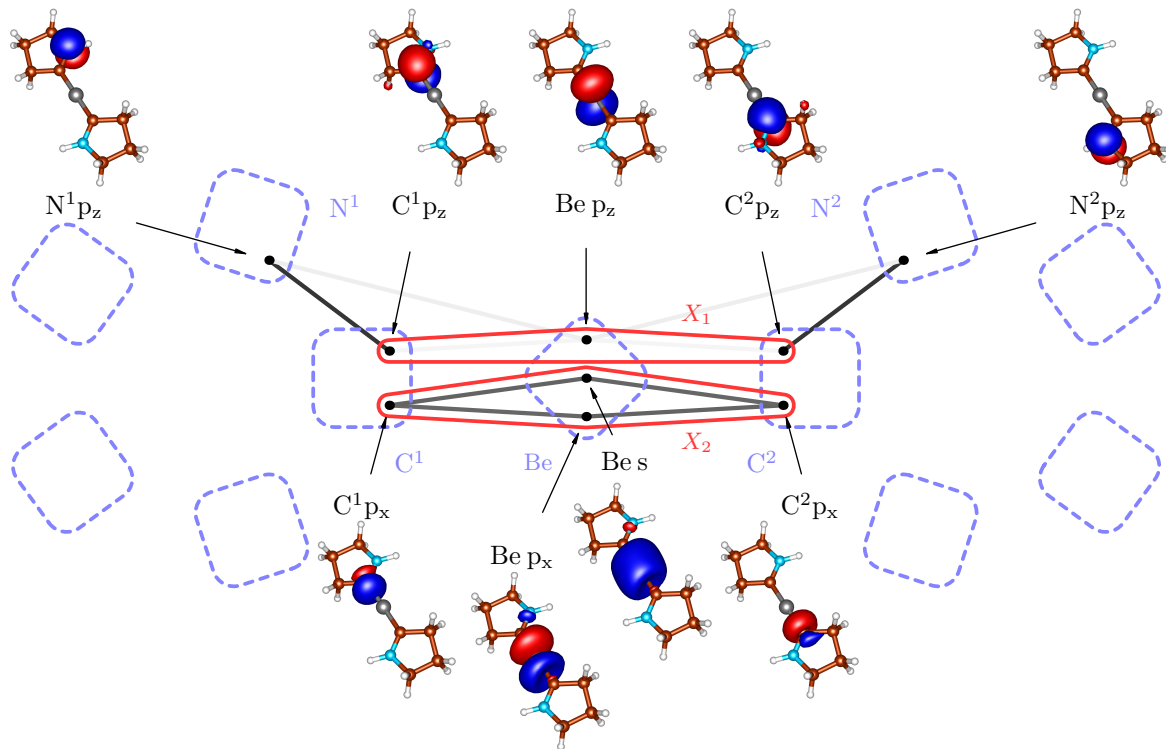


FIG. 7: Schematic view of $[\text{Be}(\text{CAC})_2]^{2+}$ with mutual information. Note that one ring is artificially flipped for clearer correlation picture.

originally doubly filled N p_z orbitals and empty C p_z orbitals. The existence of these π bonds is also confirmed by almost perfectly planar environment with the dihedral angle $\alpha_{\text{H-N-C-Be}} = 1.26^\circ$. Note that in Figure 7, we can see only the part of the double bond corresponding to the π bond - the σ bonds along the rings are excluded from the active space.

Let us now turn to the X_2 cluster of $\text{Be}(\text{CAC})_2$, i.e. to the σ bonding. The correlation of X_2 with the remaining orbitals is insignificant, however splitting of the four-orbital cluster into two σ bonds is not possible in this basis. It may therefore seem that the correct σ bond is also multiorbital. It is, however, only the artefact of the atomic-like basis, which was used in order to directly compare with Ref. 41. By simple rotation of Be s and p_x orbitals (forming the sp hybrids as in case of diboranes), one can form two independent σ bonds, essentially without influencing the rest of the system, which can be seen in Figure 8. Note that in the correlation theory of the chemical bond, superposing orbitals is allowed if this does not affect their locality too much. So superposing orbitals on different atoms is usually forbidden, while doing the same on a given atom is allowed.

Last but not least, we would like to compare the strength of both contributions to the bonding of the C-Be-C core, namely the π bond (clusters X_1 and X'_1)

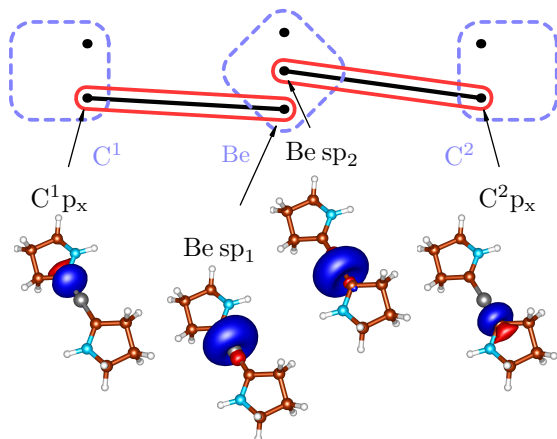


FIG. 8: Mutual information of the $\text{Be}(\text{CAC})_2$ σ bonding channel after the rotation of Be s and Be p_x orbitals.

and the σ bond (cluster X_2). In the previous study⁴¹, it was shown by means of the energy decomposition analysis combined with natural orbitals for chemical valence (EDA-NOCV)⁹⁵ that the π bonding channel is considerably more energy stabilizing than the σ channel. Let us now check the strength of both contributions by means of the correlations.

When using the more rough (three-orbital two-electron) description of the π bond (cluster X_1) and by looking at Table III, one can see on the values of C_{2-part} that σ bonds are considerably stronger than the π bond. The situation, however, dramatically changes when we use more accurate conjugated description (cluster X'_1). Note that since we are not interested in a split dissecting N and C, (because the N-C bond on the ring is stabilized by another σ bond, not visible on the plots), we have to consider the p_z orbitals together on N and C atoms of the same ring, and calculate $C_{2-part}(N^1p_z, C^1p_z | Be p_z | N^2p_z, C^2p_z)$, which turns out to be $C(N^1p_z, C^1p_z | \text{rest of } X'_1)$. Also note that in this paragraph we compared the absolute values of the correlation measures, because the clusters are of different sizes.

In Table III, one can see that the more accurate description of the π bond (X'_1) makes it of a similar strength as the σ bonds (1.737 vs 1.936). We believe that our results describe the nature of a $Be(CAC)_2$ bonding reliably, especially because we have used the genuine multireference description unlike in Ref. 41, where the analysis was based on the density functional theory (BP86 functional). We would also like to note that we have studied slightly different system than in Ref. 41. In our case all substituents were replaced by hydrogen atoms. This, however, should not influence the electronic structure of the C-Be-C core. Also note that using the s and p_x orbitals on beryllium in X_2 was only for the purpose of comparison with the previous study⁴¹. For having a more physical picture, we should use the hybridized orbitals (Figure 8), by which X_2 consists of two simple covalent bonds. Then, in order to characterize the strength of the bond, we would have to consider the Be sp_1 and sp_2 orbitals together and calculate $C_{2-part}(C^1p_x | Be sp_1, Be sp_2 | C^2p_x) = 1.935$. Nevertheless, since this value is nearly identical to $C_{2-part}(X_2)$, the conclusion is the same.

CONCLUSIONS

In this article, we have reviewed the recently developed correlation theory of the chemical bond²⁶ and applied it on molecules with multicenter electron-deficient bonds. We have demonstrated the usefulness of our methodology in characterizing molecular bonding properties by fingerprints of correlations among individual orbitals which

form these types of bonds.

We have verified the computational procedure on a textbook molecule with electron-deficient bonds, namely diborane(6), and further characterized bonding in diborane(4) and zero-valent complexes of beryllium with intricate bonding patterns. In all the cases, our results fit well with known bonding pictures or previous theoretical predictions. We have therefore proved capabilities of our new method to reliably describe bonding in complex molecular systems.

In case of the $Be(CAC)_2$ molecule, we have also compared both contributions to the C-Be-C bonding (σ and π), finding, in contrast to the previous study⁴¹, the σ and π contributions of a similar strength, in the sense of correlational quantities. We believe that our result is reliable and attribute the discrepancy with the previous study to the single reference description employed in Ref. 41, which may not be accurate enough in this multireference case.

Finally, we would like to note that, despite employing the DMRG method^{35,36} for calculations of subsystem reduced density matrices, the theory presented in this article is general and other correlated methods can in principle be employed as well¹⁶. Especially in cases of large molecules with the electronic structure dominated by the dynamical correlation for which the DMRG description may be unnecessary and computationally prohibitive.

ACKNOWLEDGEMENTS

This work has been supported by the *Czech Science Foundation* (grants no. 16-12052S, 18-24563S, and 18-18940Y), *Czech Ministry of Education, Youth and Sports* (project no. LTAUSA17033), and the *Hungarian-Czech Joint Research Project MTA/16/05*. G.B., Sz.Sz. and Ö.L. are supported by the National Research, Development and Innovation Fund of Hungary (NRDIFH) within the Researcher-initiated Research Program (project Nr: NKFIH-K120569) and the “*Lendület*” Program of the Hungarian Academy of Sciences (HAS). Sz.Sz. and Ö.L. are supported by the Quantum Technology National Excellence Program (project Nr: 2017-1.2.1-NKP-2017-00001) of NRDIFH. G.B. and Sz.Sz. are also supported by the “*Bolyai*” Research Scholarship of HAS. Ö.L. also acknowledges financial support from the Alexander von Humboldt foundation.

* jan.brandejs@jh-inst.cas.cz

† libor.veis@jh-inst.cas.cz

‡ szalay.szilard@wigner.mta.hu

§ barcza.gergely@wigner.mta.hu

¶ jiri.pittner@jh-inst.cas.cz

** legeza.ors@wigner.mta.hu

¹ Ö. Legeza and J. Sólyom, *Phys. Rev. B* **68**, 195116 (2003).

² Ö. Legeza and J. Sólyom, *Phys. Rev. B* **70**, 205118 (2004).

³ Z. Huang and S. Kais, *Chemical Physics Letters* **413**, 1 (2005).

⁴ J. Rissler, R. M. Noack, and S. R. White, *Chem. Phys.* **323**, 519 (2006).

⁵ J. Pipek and I. Nagy, *Phys. Rev. A* **79**, 052501 (2009).

- ⁶ G. Barcza, Ö. Legeza, K. H. Marti, and M. Reiher, *Phys. Rev. A* **83**, 012508 (2011).
- ⁷ L. K. McKemmish, R. H. McKenzie, N. S. Hush, and J. R. Reimers, *The Journal of Chemical Physics* **135**, 244110 (2011), 10.1063/1.3671386.
- ⁸ K. Boguslawski, K. H. Marti, O. Legeza, and M. Reiher, *J. Chem. Theory Comput.* **8**, 1970 (2012).
- ⁹ K. Boguslawski, P. Tecmer, Örs Legeza, and M. Reiher, *J. Phys. Chem. Lett.* **3**, 3129 (2012).
- ¹⁰ K. Boguslawski, P. Tecmer, G. Barcza, Ö. Legeza, and M. Reiher, *Journal of Chemical Theory and Computation* **9**, 2959 (2013).
- ¹¹ Y. Kurashige, G. K.-L. Chan, and T. Yanai, *Nature Chemistry* **5**, 660 (2013).
- ¹² E. Fertitta, B. Paulus, G. Barcza, and Ö. Legeza, *Phys. Rev. B* **90**, 245129 (2014).
- ¹³ C. Duperrouzel, P. Tecmer, K. Boguslawski, G. Barcza, Ö. Legeza, and P. W. Ayers, *Chemical Physics Letters* **621**, 160 (2015).
- ¹⁴ V. Murg, F. Verstraete, R. Schneider, P. R. Nagy, and O. Legeza, *J. Chem. Theory Comput.* **11**, 1027 (2015).
- ¹⁵ S. Knecht, Örs Legeza, and M. Reiher, *The Journal of Chemical Physics* **140**, 041101 (2014).
- ¹⁶ K. Boguslawski and P. Tecmer, *International Journal of Quantum Chemistry* **115**, 1289 (2015).
- ¹⁷ Sz. Szalay, M. Pfeiffer, V. Murg, G. Barcza, F. Verstraete, R. Schneider, and Ö. Legeza, *Int. J. Quantum Chem.* **115**, 1342 (2015).
- ¹⁸ L. Freitag, S. Knecht, S. F. Keller, M. G. Delcey, F. Aquilante, T. Bondo Pedersen, R. Lindh, M. Reiher, and L. Gonzalez, *Phys. Chem. Chem. Phys.* **17**, 14383 (2015).
- ¹⁹ Y. Zhao, K. Boguslawski, P. Tecmer, C. Duperrouzel, G. Barcza, Ö. Legeza, and P. W. Ayers, *Theor. Chem. Acc.* **134**, 120 (2015).
- ²⁰ T. Szilvási, G. Barcza, and Ö. Legeza, *arXiv [physics.chem-ph]*, 1509.04241 (2015).
- ²¹ M. Molina-Espíritu, R. O. Esquivel, S. López-Rosa, and J. S. Dehesa, *Journal of Chemical Theory and Computation* **11**, 5144 (2015).
- ²² C. Krumnow, L. Veis, O. Legeza, and J. Eisert, *Phys. Rev. Lett.* **117**, 210402 (2016).
- ²³ C. J. Stein and M. Reiher, *J. Chem. Theory Comput.* **12**, 1760 (2016).
- ²⁴ C. Stein and M. Reiher, *Chimia* **71**, 170 (2017).
- ²⁵ A. Kovyrshin and M. Reiher, *J. Chem. Phys.* **147**, 214111 (2017).
- ²⁶ Sz. Szalay, G. Barcza, T. Szilvási, L. Veis, and Ö. Legeza, *Scientific Reports* **7**, 2237 (2017).
- ²⁷ C. Stemmler, B. Paulus, and Örs Legeza, *Physical Review A* **97** (2018), 10.1103/physreva.97.022505.
- ²⁸ Y. Kurashige and T. Yanai, *The Journal of Chemical Physics* **130**, 234114 (2009), 10.1063/1.3152576.
- ²⁹ V. Murg, F. Verstraete, O. Legeza, and R. M. Noack, *Physical Review B* **82** (2010), 10.1103/physrevb.82.205105.
- ³⁰ N. Nakatani and G. K.-L. Chan, *The Journal of Chemical Physics* **138**, 134113 (2013).
- ³¹ G. K.-L. Chan, A. Kesselman, N. Nakatani, Z. Li, and S. R. White, *The Journal of Chemical Physics* **145**, 014102 (2016).
- ³² S. Keller, M. Dolfi, M. Troyer, and M. Reiher, *The Journal of Chemical Physics* **143**, 244118 (2015).
- ³³ S. Wouters and D. Van Neck, *The European Physical Journal D* **68**, 272 (2014), 10.1140/epjd/e2014-50500-1.
- ³⁴ K. Gunst, F. Verstraete, S. Wouters, Örs Legeza, and D. V. Neck, *Journal of Chemical Theory and Computation* **14**, 2026 (2018).
- ³⁵ S. R. White, *Phys. Rev. Lett.* **69**, 2863 (1992).
- ³⁶ S. R. White, *Phys. Rev. B* **48**, 10345 (1993).
- ³⁷ U. Schollwöck, *Ann. Phys.* **326**, 96 (2011).
- ³⁸ F. M. Faulstich, M. Mt, A. Laestadius, M. A. Csirik, L. Veis, A. Antalik, J. Brabec, R. Schneider, J. Pittner, S. Kvaal, and rs Legeza, “Numerical and theoretical aspects of the dmrg-tcc method exemplified by the nitrogen dimer,” (2018), [arXiv:1809.07732](https://arxiv.org/abs/1809.07732).
- ³⁹ The number in parentheses denotes the number of hydrogen atoms.
- ⁴⁰ S.-L. Chou, J.-I. Lo, Y.-C. Peng, M.-Y. Lin, H.-C. Lu, B.-M. Cheng, and J. F. Ogilvie, *Chemical Science* **6**, 6872 (2015).
- ⁴¹ M. Arrowsmith, H. Braunschweig, M. A. Celik, T. Dellermann, R. D. Dewhurst, W. C. Ewing, K. Hammond, T. Kramer, I. Krummenacher, J. Mies, K. Radacki, and J. K. Schuster, *Nature Chemistry* **8**, 890 (2016).
- ⁴² J. Brabec, J. Lang, M. Saitow, J. Pittner, F. Neese, and O. Demel, *J. Chem. Theor. Comput.* **14**, 1370 (2018).
- ⁴³ H. C. Longuet-Higgins, *Journal of the Chemical Society (Resumed)*, 139 (1946).
- ⁴⁴ H. C. Longuet-Higgins and R. P. Bell, *Journal of the Chemical Society (Resumed)*, 250 (1943).
- ⁴⁵ W. H. Eberhardt, B. Crawford, and W. N. Lipscomb, *The Journal of Chemical Physics* **22**, 989 (1954).
- ⁴⁶ K. Lammertsma and T. Ohwada, *Journal of the American Chemical Society* **118**, 7247 (1996).
- ⁴⁷ W. N. Lipscomb, *Accounts of Chemical Research* **6**, 257 (1973).
- ⁴⁸ E. C. Neeve, S. J. Geier, I. A. I. Mkhaliid, S. A. Westcott, and T. B. Marder, *Chemical Reviews* **116**, 9091 (2016).
- ⁴⁹ M. A. Vincent and H. F. Schaefer, *Journal of the American Chemical Society* **103**, 5677 (1981).
- ⁵⁰ R. R. Mohr and W. N. Lipscomb, *Inorganic Chemistry* **25**, 1053 (1986).
- ⁵¹ L. A. Curtiss and J. A. Pople, *The Journal of Chemical Physics* **90**, 4314 (1989).
- ⁵² L. A. Curtiss and J. A. Pople, *The Journal of Chemical Physics* **91**, 5118 (1989).
- ⁵³ I. Demachy and F. Volatron, *The Journal of Physical Chemistry* **98**, 10728 (1994).
- ⁵⁴ I. Alkorta, I. Soteras, J. Elguero, and J. E. D. Bene, *Physical Chemistry Chemical Physics* **13**, 14026 (2011).
- ⁵⁵ P. P. Power, *Nature* **463**, 171 (2010).
- ⁵⁶ P. P. Power, *The Chemical Record* **12**, 238 (2011).
- ⁵⁷ N. A. Giffin and J. D. Masuda, *Coordination Chemistry Reviews* **255**, 1342 (2011).
- ⁵⁸ M. Niemeyer and P. P. Power, *Inorganic Chemistry* **36**, 4688 (1997).
- ⁵⁹ D. Naglav, A. Neumann, D. Bläser, C. Wölper, R. Haack, G. Jansen, and S. Schulz, *Chemical Communications* **51**, 3889 (2015).
- ⁶⁰ T. Arnold, H. Braunschweig, W. C. Ewing, T. Kramer, J. Mies, and J. K. Schuster, *Chemical Communications* **51**, 737 (2015).
- ⁶¹ H.-W. Lerner, S. Scholz, M. Bolte, N. Wiberg, H. Nöth, and I. Krossing, *European Journal of Inorganic Chemistry* **2003**, 666 (2003).

- ⁶² K. C. Mondal, H. W. Roesky, M. C. Schwarzer, G. Frenking, B. Niepötter, H. Wolf, R. Herbst-Irmer, and D. Stalke, *Angewandte Chemie International Edition* **52**, 2963 (2013).
- ⁶³ Y. Li, K. C. Mondal, H. W. Roesky, H. Zhu, P. Stollberg, R. Herbst-Irmer, D. Stalke, and D. M. Andrada, *Journal of the American Chemical Society* **135**, 12422 (2013).
- ⁶⁴ Sz. Szalay, *Phys. Rev. A* **92**, 042329 (2015).
- ⁶⁵ M. Ohya and D. Petz, *Quantum Entropy and Its Use*, 1st ed. (Springer Verlag, 1993).
- ⁶⁶ H. Araki and H. Moriya, *Reviews in Mathematical Physics* **15**, 93 (2003).
- ⁶⁷ M. M. Wilde, *Quantum Information Theory* (Cambridge University Press, 2013).
- ⁶⁸ R. Horodecki, P. Horodecki, M. Horodecki, and K. Horodecki, *Rev. Mod. Phys.* **81**, 865 (2009).
- ⁶⁹ E. Schrödinger, *Math. Proc. Camb. Phil. Soc.* **32**, 446 (1936).
- ⁷⁰ L. P. Hughston, R. Jozsa, and W. K. Wootters, *Phys. Lett. A* **183**, 14 (1993).
- ⁷¹ B. A. Davey and H. A. Priestley, *Introduction to Lattices and Order*, 2nd ed. (Cambridge University Press, 2002).
- ⁷² Sz. Szalay and Z. Kökényesi, *Phys. Rev. A* **86**, 032341 (2012).
- ⁷³ S. Szalay, *Journal of Physics A: Mathematical and Theoretical* **51**, 485302 (2018).
- ⁷⁴ G. Adesso, T. R. Bromley, and M. Cianciaruso, *Journal of Physics A: Mathematical and Theoretical* **49**, 473001 (2016).
- ⁷⁵ Ö. Legeza and J. Sólyom, *Phys. Rev. Lett.* **96**, 116401 (2006).
- ⁷⁶ J. Rissler, R. M. Noack, and S. R. White, *Chemical Physics* **323**, 519 (2006).
- ⁷⁷ M. Mottet, P. Tecmer, K. Boguslawski, Ö. Legeza, and M. Reiher, *Phys. Chem. Chem. Phys.* **16**, 8872 (2014).
- ⁷⁸ V. Murg, F. Verstraete, R. Schneider, P. R. Nagy, and Ö. Legeza, *Journal of Chemical Theory and Computation* **11**, 1027 (2015).
- ⁷⁹ G. Barcza, R. M. Noack, J. Sólyom, and Ö. Legeza, *Phys. Rev. B* **92**, 125140 (2015).
- ⁸⁰ G. Lindblad, *Communications in Mathematical Physics* **33**, 305 (1973).
- ⁸¹ R. Horodecki, *Physics Letters A* **187**, 145 (1994).
- ⁸² Ö. Legeza, F. Gebhard, and J. Rissler, *Phys. Rev. B* **74**, 195112 (2006).
- ⁸³ F. Herbut, *Journal of Physics A: Mathematical and General* **37**, 3535 (2004).
- ⁸⁴ K. Modi, T. Paterek, W. Son, V. Vedral, and M. Williamson, *Phys. Rev. Lett.* **104**, 080501 (2010).
- ⁸⁵ C. H. Bennett, H. J. Bernstein, S. Popescu, and B. Schumacher, *Phys. Rev. A* **53**, 2046 (1996).
- ⁸⁶ M. A. Nielsen and I. L. Chuang, *Quantum Computation and Quantum Information*, 1st ed. (Cambridge University Press, 2000).
- ⁸⁷ E. Schmidt, *Math. Ann.* **63**, 433 (1907).
- ⁸⁸ J. Pipek and P. G. Mezey, *The Journal of Chemical Physics* **90**, 4916 (1989).
- ⁸⁹ H. J. Werner, P. J. Knowles, G. Knizia, F. R. Manby, and M. Schütz, “Molpro, version 2010.1, a package of ab initio programs, <http://www.molpro.net>,” (2010).
- ⁹⁰ Ö. Legeza, L. Veis, and T. Mosoni, “QC-DMRG-Budapest, a program for quantum chemical DMRG calculations,”
- ⁹¹ J. Chalupsky, “Charmol: program for molecular graphics,” <https://sourceforge.net/projects/charmol>, accessed: 2018-09-09.
- ⁹² T. J. Osborne and F. Verstraete, *Physical Review Letters* **96** (2006), 10.1103/physrevlett.96.220503.
- ⁹³ V. Coffman, J. Kundu, and W. K. Wootters, *Physical Review A* **61** (2000), 10.1103/physreva.61.052306.
- ⁹⁴ T. Szilvasi, G. Barcza, and O. Legeza, *arXiv [quant-ph]*, 1509.04241 (2015).
- ⁹⁵ A. Krapp, K. K. Pandey, and G. Frenking, *J. Am. Chem. Soc.* **129**, 7596 (2007).

Appendix A: Eigenvectors of the reduced density operators

1. Be(CAC)₂

The (reduced) density operator of the X_1 orbitals consists of the following eigenstates of the three highest eigenvalues (probabilities).

Probability 0.5798:

$$\begin{aligned} |\psi_{X_1}^1\rangle = & + 0.0864 |-- \uparrow \downarrow\rangle + 0.3255 |-\downarrow \uparrow\rangle - 0.3255 |-\uparrow \downarrow\rangle \\ & + 0.3324 |-\uparrow \downarrow -\rangle + 0.4748 |\downarrow - \uparrow\rangle - 0.3254 |\downarrow \uparrow -\rangle \\ & - 0.4748 |\uparrow - \downarrow\rangle + 0.3254 |\uparrow \downarrow -\rangle + 0.0863 |\uparrow \downarrow --\rangle \end{aligned}$$

Probability 0.1473:

$$\begin{aligned} |\psi_{X_1}^2\rangle = & - 0.2010 |-\downarrow \uparrow \downarrow\rangle - 0.2630 |-\uparrow \downarrow \downarrow\rangle - 0.3980 |\downarrow - \uparrow \downarrow\rangle \\ & - 0.2781 |\downarrow \downarrow \uparrow\rangle + 0.5562 |\downarrow \uparrow \downarrow\rangle - 0.2630 |\downarrow \uparrow \downarrow -\rangle \\ & - 0.2781 |\uparrow \downarrow \downarrow\rangle - 0.3980 |\uparrow \downarrow - \downarrow\rangle + 0.2010 |\uparrow \downarrow \downarrow -\rangle \end{aligned}$$

Probability 0.1473:

$$\begin{aligned} |\psi_{X_1}^3\rangle = & + 0.2010 |-\uparrow \uparrow \downarrow\rangle + 0.2630 |-\uparrow \downarrow \uparrow\rangle - 0.2781 |\downarrow \uparrow \uparrow\rangle \\ & + 0.3980 |\uparrow - \uparrow \downarrow\rangle + 0.5562 |\uparrow \downarrow \uparrow\rangle - 0.2781 |\uparrow \uparrow \downarrow\rangle \\ & + 0.2630 |\uparrow \uparrow \downarrow -\rangle + 0.3980 |\uparrow \downarrow - \uparrow\rangle - 0.2010 |\uparrow \downarrow \uparrow -\rangle \end{aligned}$$

all the other eigenvalues are less than 0.033.

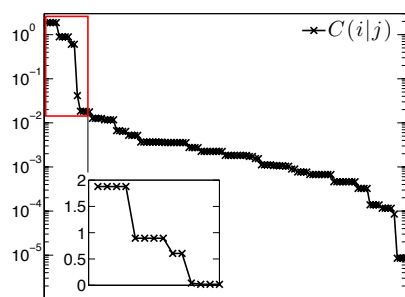
2. [Be(CAC)₂]²⁺

As mentioned earlier in the text, the reduced density operator for X_1 is highly mixed in this case, with no dominant state. Therefore we only list the highest eigenvalues to show this:

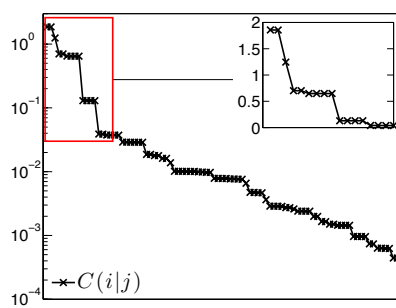
$$\begin{aligned} & 0.1016, 0.1007, 0.1007, 0.1007, 0.1002, \\ & 0.1002, 0.0899, 0.0899, 0.0868, 0.0214. \end{aligned}$$

3. Distribution of the two-orbital correlations

Figure 9 shows the distribution of the two-orbital correlations for diborane and beryllium complexes.



(a) diborane(6)



(b) diborane(4)

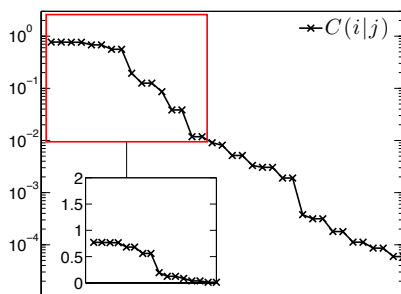
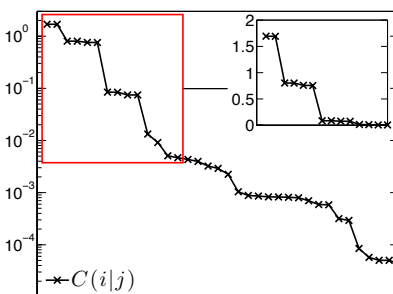
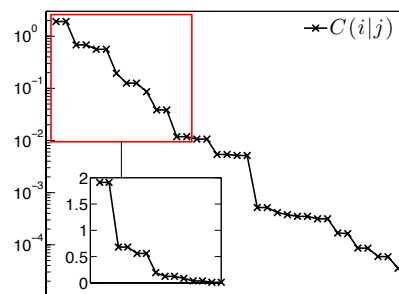
(c) Be(CAC)₂(d) [Be(CAC)₂]²⁺(e) Be(CAC)₂ with rotated X_2

FIG. 9: The distributions of the two-orbital correlations for diborane and beryllium complexes.